

# Matrix Isolation and Computational Studies of Benzoyl Chloride Photolysis

**Nobuaki Tanaka<sup>1\*</sup>**

<sup>1</sup>*Department of Environmental Science and Technology, Faculty of Engineering, Shinshu University, 4-17-1 Wakasato, Nagano 380-8553, Japan.*

## *Author's contribution*

*This whole work was carried out by the author NT.*

**Original Research Article**

**Received 4<sup>th</sup> June 2014**

**Accepted 30<sup>th</sup> June 2014**

**Published 14<sup>th</sup> July 2014**

## **ABSTRACT**

The UV light photolysis ( $\lambda > 260$  nm) of benzoyl chloride was investigated using matrix isolation FT-IR spectroscopy and computational methods (MP2, B3LYP, CCSD, and SAC-Cl). The photolysis products were found to be chlorobenzene and CO. An intermediate species was identified with 6-chloro-2, 4-cyclohexadien-1-ylidemethanone (CCHM) from the MP2 calculations. Changes in the CCHM absorption bands showed a typical growth and decay profile for an intermediate species in a consecutive reaction. In addition, 6-chlorofulvene was found to be a minor product.

**Keywords:** Benzoyl chloride; photolysis; cryogenic matrix; MP2; B3LYP.

## **1. INTRODUCTION**

Benzoyl chloride (BC) is an important reagent in organic synthesis. Due to its high reactivity, BC is used as a reactant in the synthesis of benzoic acid derivatives and as an acylation reagent of aromatic compounds [1]. It is also used in the polymer manufacturing industry as a reinforcement reagent for thermoplastic resins [2] and as a surface modification reagent for fibers [3].

\*Corresponding author: Email: ntanaka@shinshu-u.ac.jp;

Among the acyl chloride compounds, acetyl chloride has attracted much attention from the standpoint of its photolysis. In the gas phase, the rapid C–Cl bond dissociation occurs in the excited singlet state following the  $^1(n, \pi^*)$  excitation, followed by the  $\text{CH}_3\text{CO}$  fragmentation into  $\text{CH}_3$  and CO [4-6]. In the rare gas matrices, the concerted HCl elimination occurs to yield the  $\text{HCl}\cdots\text{ketene}$  complex in the ground state following the internal conversion from the  $S_1$  state [7]. Recently, Saha et al. studied the photolysis of gas phase BC at a wavelength of 235 nm [8]. The predominant (72%) high kinetic energy C–Cl dissociation channel arises from the  $S_1$  state having  $n\pi^*$  character of BC. The minor low kinetic energy C–Cl bond dissociation channel and the HCl molecular channel originate from the ground electronic state of BC, after nonradiative relaxation of the initially excited state. In a previous study on the *o*-chlorobenzaldehyde photolysis in an Ar matrix using a wavelength of 185 nm, we found that *o*-chlorobenzaldehyde was photo rearranged to form BC [9]. The photoproduct BC was further decomposed to form chlorobenzene and CO through an intermediate species. Judging from the growth behaviors of the  $2120\text{ cm}^{-1}$  band of the intermediate and the  $2138\text{ cm}^{-1}$  band of the CO product, the intermediate species was tentatively identified with 6-chloro-2,4-cyclohexadien-1-ylidenemethanone (CCHM). The photodissociation of BC when it was irradiated at a wavelength of 185 nm was found to result in a benzoyl radical and a Cl radical. These products recombined in the matrix cage to yield CCHM.

In the present study, the UV photolysis of BC in a low-temperature Ar matrix was investigated using a longer excitation wavelength to minimize the further decomposition of the product. The product spectra were compared with spectra that were computationally obtained. A possible reaction mechanism was identified using the calculated potential energies.

## 2. EXPERIMENTAL DETAILS

BC, which was obtained from Wako Pure Chemical Industries (Osaka, Japan) was purified by trap-to-trap distillation under vacuum and diluted with argon (99.999 % purity; Nippon Sanso, Tokyo, Japan) to about 1/1000 (0.2 TorrBC and 200 TorrAr). The BC/Ar mixture was slowly sprayed on a CsI plate that was cooled to about 7 K by a closed-cycle helium refrigerator (Iwatani CryoMini M310/CW303). Infrared absorption spectra were measured using a Shimadzu FTIR 8300 spectrophotometer equipped with an MCT detector. The effect of photoexciting BC was examined by irradiating deposited samples for 330 min with UV light. A Xe short arc lamp (Hamamatsu, C2577) was used as UV light source combined with a water filter to remove thermal radiation and a bandpass filter (HOYA, U340,  $260\text{ nm} < \lambda < 380\text{ nm}$ ). UV–Vis absorption spectra were measured using a Shimadzu UV-3150 spectrophotometer.

Quantum chemical calculations were carried out using the GAUSSIAN 09 program [10]. Optimized geometries, wavenumbers, and infrared absorption intensities were obtained using B3LYP [11] and MP2 calculations. The vertical transition energies of the parent and intermediate species were calculated at the SAC-Cl/D95+(d, p) level based on the structures optimized at the CCSD/D95+(d, p) level.

## 3. RESULTS AND DISCUSSION

### 3.1 Identification of Products

The BC/Ar(1/1000) mixture deposited on the CsI window resulted in strong IR absorption bands at  $1794$  and  $886\text{ cm}^{-1}$ , which can be assigned to C=O and C–Cl stretching vibrations

of BC, respectively [12]. The spectrum was well reproduced by the calculated spectral pattern at the MP2/6-311++G(2d,2p) level. An IR difference spectrum obtained by subtracting the spectrum measured before UV irradiation from that measured after a sample was irradiated with UV for 15 min (15–0) is shown in Fig. 1a. An IR difference spectrum obtained by subtracting the spectrum measured after irradiating a sample with UV for 60 min from that measured after irradiating a sample with UV for 330 min (330–60) is shown in Fig. 1c. The positive and negative bands indicate growth and depletion, respectively, during the irradiation period. Irradiation resulted in a decrease in the intensities of the bands caused by absorption by the reactant, BC, and the appearance of new bands (shown in Fig. 1a). The bands that increased in intensity were classified into three groups (species A, B, and C) by their different growth behaviors. The absorption bands caused by species A were found to decrease in intensity with increasing irradiation time (shown in Fig. 1c), while the absorption bands caused by species B and C continued to grow during the prolonged irradiation period. Table 1 lists the wavenumbers of the products. The evolutions of the integrated band intensities of BC, species A, species B and the band at 2137 cm<sup>-1</sup> over time are shown in Fig. 2. The species A absorption bands reached a maximum at an irradiation time of approximately 60 min and then started to decrease. The integrated band intensities suggest that species B and the species resulting in the band at 2137 cm<sup>-1</sup> were consecutively produced through the degradation of intermediate species A. The band at 2120 cm<sup>-1</sup> caused by species A, was previously observed when BC was irradiated with a wavelength of 185 nm. Five bands at 1186, 960, 786, 735 and 705 cm<sup>-1</sup> showed the same growth behavior as the band at 2120 cm<sup>-1</sup>; this behavior was dominant in the early stages of the irradiation process. Ketene species shows strong C=C=O asymmetric stretching vibrations at approximately 2140 cm<sup>-1</sup>. Therefore, the wavenumbers and intensities that were found were compared with those for CCHM calculated at the MP2/6-311++G(2d,2p) level (Fig. 1b). The calculated spectrum reproduced the observed spectrum well. Species A was therefore identified with CCHM. The band at 2137 cm<sup>-1</sup> was assigned to the stretching vibration of CO. The wavenumbers for species B agree with those for chlorobenzene. The bands at 1481, 1448, 1088, 1024, 740, and 705 cm<sup>-1</sup> were assigned to the C–C stretching, C–C stretching, C–H in-plane bending, C–H in-plane bending, C–H out-of-plane bending, and CCC in-plane bending vibrations of chlorobenzene, respectively [13]. The relative intensities of the bands at 740 and 705 cm<sup>-1</sup> caused by chlorobenzene in Figs. 1a and 1c, respectively, are different. Comparing the intensity of the band at 705 cm<sup>-1</sup> in Fig. 1a with the authentic spectrum of chlorobenzene in Ar showed that the band in Fig. 1a was too large for it to be solely caused by chlorobenzene. An absorption band caused by CCHM was found to overlap with the band at 705 cm<sup>-1</sup> caused by chlorobenzene. The irradiation of BC at  $\lambda > 260$  nm yielded chlorobenzene, as irradiation at  $\lambda = 185$  nm did [9]. Ketene can be photolyzed to form carbene and CO in the S<sub>1</sub> and T<sub>1</sub> states. By analogy, we assumed that CCHM could also photodecompose to form carbene and CO. The reactive carbene may be rearranged to form chlorobenzene. From the growth of the absorption bands, it appears that species C is the photoproduct of species B. The band at 1624 cm<sup>-1</sup> was in the C=C stretching vibration region. Nagata et al. suggested that the ketocarbene species acts as a reactive intermediate species, which rearranges to form cyclopentadienylidenemethanone during the photolysis of 2-iodophenol in an Ar matrix [14]. In this study, carbene may also have rearranged to form 6-chlorofulvene (CF). The wavenumbers and intensities of the absorption bands caused by species C were compared with those for CF calculated at the MP2/6-311++G(2d,2p) level (Fig. 1d). The calculated wavenumbers well reproduced the observed spectrum. Therefore, species C was identified with CF. The IR absorption band intensities for chlorobenzene and CF calculated at the MP2/6-311++G(2d,2p) level were used to calculate the product yield ratio,  $\phi_{\text{chlorobenzene}}/\phi_{\text{CF}}$ , from the carbene and the ratio was found to be 5.9. The formation of

chlorobenzene was found to be the major reaction path during the CCHM photolysis in the Ar matrix at the present irradiation energy.

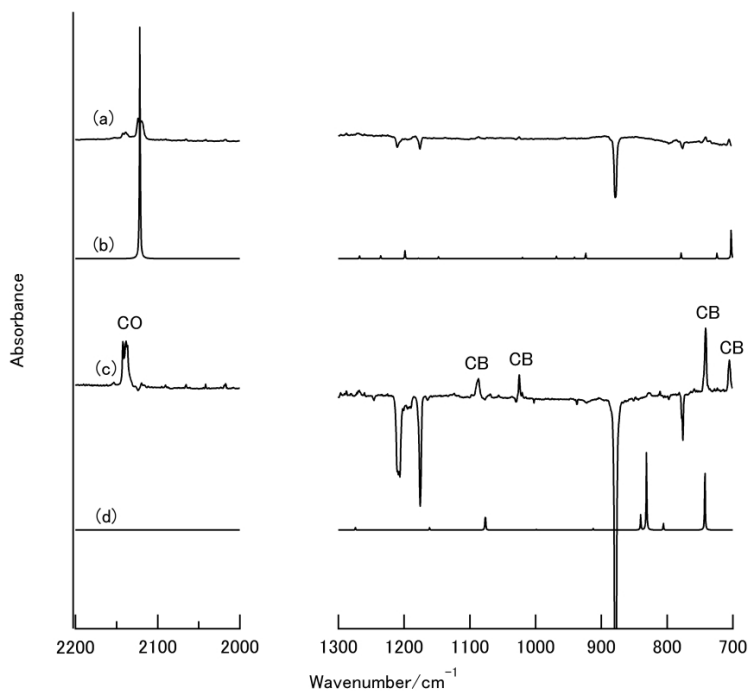


**Fig. 1.** IR difference spectra upon UV irradiation of the matrix BC/Ar = 1/1000 obtained by the spectral subtraction of (a) 15–0 min and (c) 330–60 min. Calculated spectral patterns of (b) CCHM and (d) CF at the MP2/6-311++G(2d2p) level of theory using a scaling factor of 0.98. The bands marked with CO and CB represent the absorption bands of CO and chlorobenzene, respectively

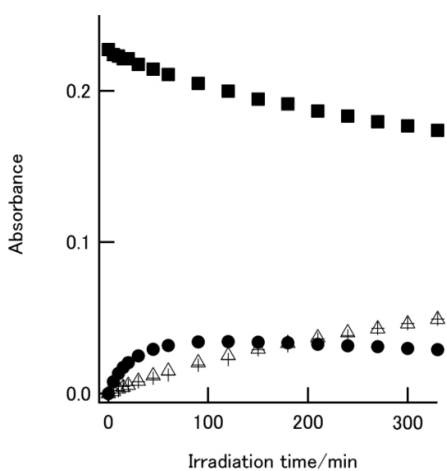


**Fig. 2.** Absorbance changes of the BC (■), CCHM (●), CO ( $\Delta$ ) and chlorobenzene(+,  
 $A_{1100\text{ cm}^{-1}} \times 3$ ) upon UV irradiation of the matrix BC/Ar = 1/1000

**Table 1. Observed and calculated wavenumbers of photochemical reaction products of BC in the Ar matrix**

obs	wavenumber/cm <sup>-1</sup>	species
	calc <sup>a</sup>	
2138		CO
2120	2123	CCHM
1624	1616	6-chlorofulvene
1544	1525	CCHM
1481		chlorobenzene
1448		chlorobenzene
1186	1199	CCHM
1088		chlorobenzene
1056	1076	6-chlorofulvene
1024		chlorobenzene
960	968	CCHM
903	912	6-chlorofulvene
828	840/832	6-chlorofulvene
811	806	6-chlorofulvene
786	779	CCHM
758	742	6-chlorofulvene
740		chlorobenzene
735	724	CCHM
705	703	CCHM, chlorobenzene

<sup>a</sup>The wavenumbers for CCHM and 6-chlorofulvene were calculated at the MP2/6-311++G(2d,2p) level. A scaling factor of 0.98 was used

### 3.2 Reaction Mechanism

Along with the absorption band caused by CO, the bands caused by chlorobenzene continued to increase with time and became the main bands seen in Fig. 1c. The proposed reaction mechanism for the photolysis of BC is shown in Scheme 1. The optimized structures of the photoproducts and transition states are shown in Fig. 3. Fig. 4 shows the energy diagram for BC photolysis calculated at the (U) B3LYP/6-311++G(3df,3pd) level. The vertical transition energies for BC were calculated at the SAC-Cl/D95+(d,p)//CCSD/D95+(d, p) level. The S<sub>1</sub> (4.29 eV), S<sub>2</sub> (4.47 eV) and S<sub>3</sub> (5.35 eV) states of BC were characterized as the nπ\* (HOMO-2 → LUMO), ππ\* (HOMO → LUMO), and πππ\* (HOMO-1 → LUMO) states, respectively, with oscillator strengths of 0.0, 0.017, and 0.31, respectively. The photon energy at a wavelength of 260 nm corresponded to 110 kcal mol<sup>-1</sup> (4.77 eV), and this energy will excite BC into the S<sub>2</sub> state. Verma et al. assigned the BC vapor absorption band at 287.18 nm to the (0,0) band [15]. In the Franck–Condon region, two triplet states, T<sub>1</sub> (3.56 eV, ππ\*) and T<sub>2</sub> (4.12 eV, nπ\*), were calculated to exist below the S<sub>1</sub> state. The carbonyl compounds are known to undergo α dissociation in both the singlet and triplet nπ\* states. Hence, BC will photodissociate to form benzoyl radical and a chlorine atom. Distinctly different benzoyl radical structures exist with respect to the geometry of the PhCO group, a linear and a bent forms. The formation of the benzoyl radical with a linear acyl group is symmetry-allowed because of the correlation between the states [16]. The energy difference between the linear and bent structures of the benzoyl radical was calculated to be 4.8 kcal mol<sup>-1</sup>, which is relatively small compared with the energy of the acetyl radical (25 kcal mol<sup>-1</sup>), and this small energy difference is caused by resonance stabilization in the linear structure. Therefore, the benzoyl radical and chlorine atom that are produced will recombine to form

CCHM in the matrix cage. Alternatively, the vibrationally excited  $S_0$  state of BC may be produced when the efficient internal conversion from the  $S_1$  state or intersystem crossing from the  $T_1$  state occurs. The calculated transition state, TS1, connecting BC in the  $S_0$  state and CCHM, has an energy of 45 kcal mol $^{-1}$ . The imaginary frequency of TS1 was calculated to be 166*i* cm $^{-1}$  at the B3LYP/6-311++G(3df,3pd) level. Ketene species can be photolyzed to form carbene and CO in the  $S_1$  and  $T_1$  states [17]. The SAC-CI calculation gave vertical transition energies of the CCHM  $S_1$ ,  $S_2$ ,  $S_3$  and  $S_4$  states of 2.55, 3.79, 4.54 and 5.28 eV, respectively. CCHM can reach the  $S_3$  state when it is irradiated at  $\lambda > 260$  nm. CCHM will then be dissociated (analogous to the dissociation of ketene species) to form carbene and CO. Calculations showed that the triplet carbene is more stable than the singlet carbene by 9.6 and 6.4 kcal mol $^{-1}$  at the B3LYP/6-311++G(3df,3pd) and CCSD/D95+(d, p) levels, respectively. We did not observe absorption bands that were assignable to carbene vibrations, so the reactive carbene species must dissociate or become rearranged. In the  $T_0$  state, the equilibrium C–Cl bond length was calculated to be quite long, 2.495 Å, and the bond dissociation energy was calculated to be 9.4 kcal mol $^{-1}$ . These parameters indicate that the C–Cl bond could dissociate in the matrix cage, so that chlorobenzene is formed during the photolysis process, and this could occur even with the excess energy present after the photolysis of CCHM. If carbene was in the singlet state, the hydrogen or chlorine atom could migrate through TS2 or TS3, respectively, and rearrangement to form chlorobenzene would occur.

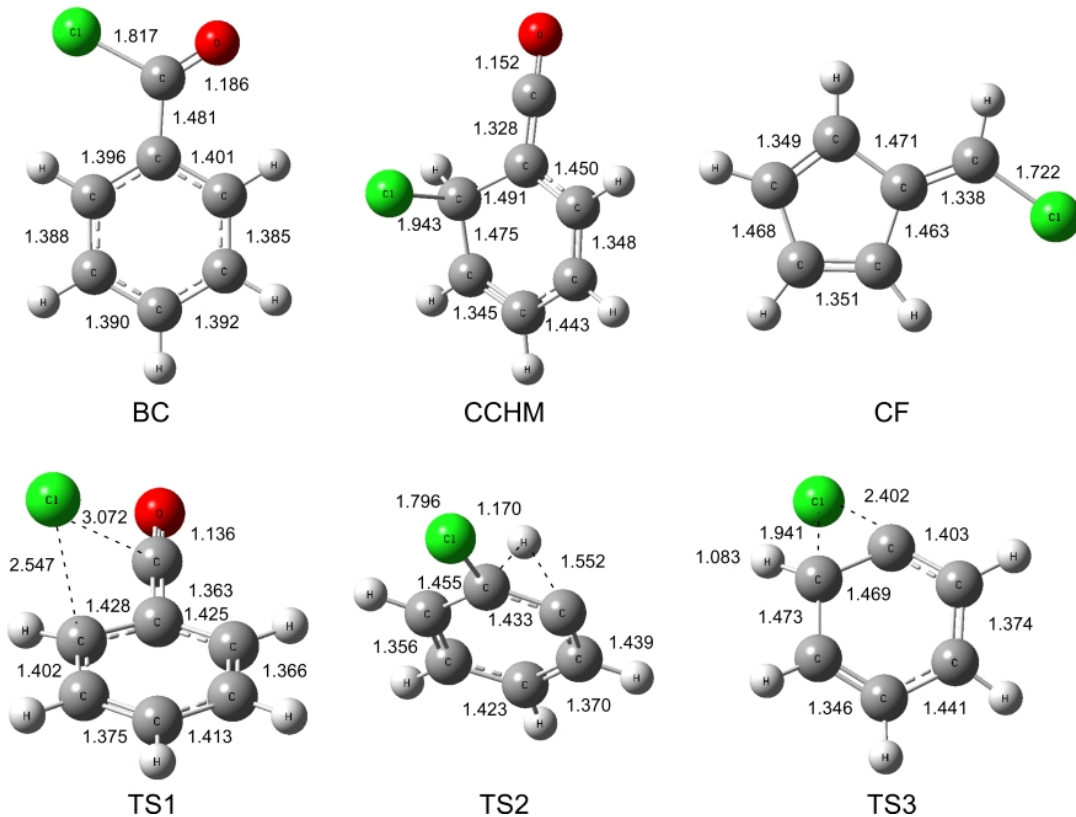
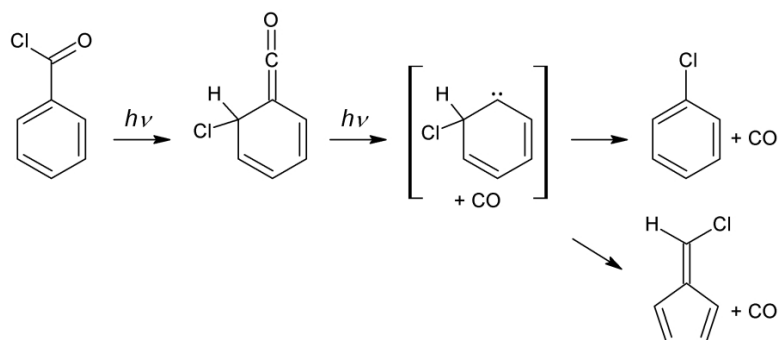


**Fig. 3. Optimized structures of photoproducts and transition states calculated at the B3LYP/6-311++G(3df, 3pd) level of theory. Bond lengths are in Å**



Scheme 1

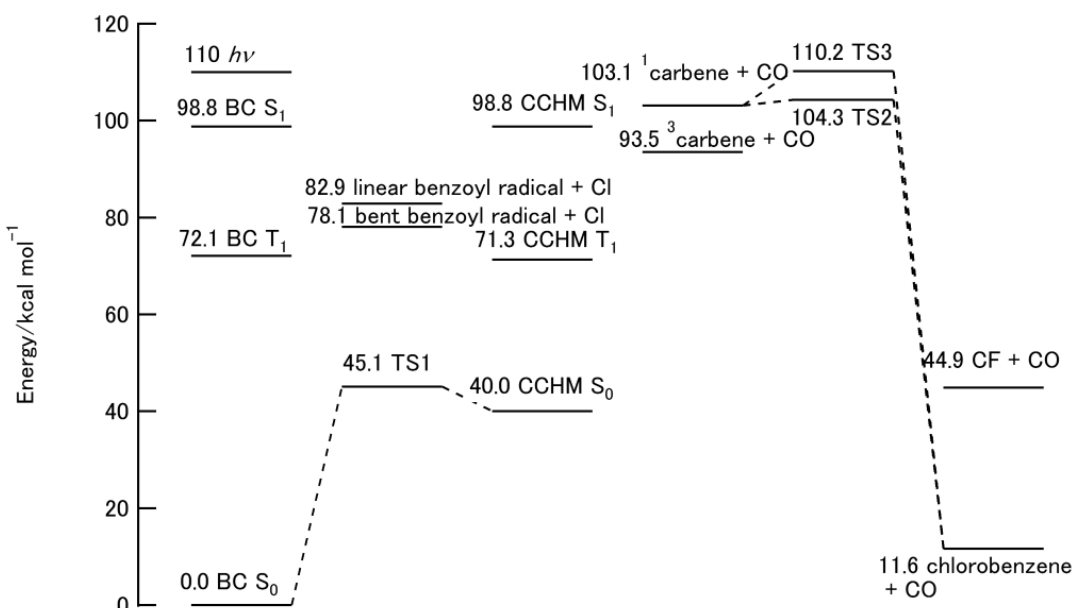


**Fig. 4. Potential energy diagram for the BC photolysis calculated at the B3LYP/6-311++G(3df,3pd) level of theory. The S<sub>1</sub> energies of BC and CCHM were the transition energies calculated at the SAC-Cl/D95+(d,p)**

#### 4. CONCLUSION

The UV-light photolysis of BC was investigated in a cryogenic Ar matrix. The photolysis products were chlorobenzene and CO. An intermediate species, CCHM, was identified from the MP2 calculations. A minor product, CF, was also observed. Three transition states were found on the reaction potentials, according to B3LYP calculations.

#### COMPETING INTERESTS

Authors have declared that no competing interests exist.

## REFERENCES

1. Solomons TWG, Fryhle CB. *Organic Chemistry* 10<sup>th</sup> ed. Hoboken: John Wiley & Sons, Inc; 2011.
2. Zakaria S, Poh LK. Polystyrene-benzoylated EFB reinforced composites. *Polymer-Plastics Tech Eng.* 2002;41(5):951-962.
3. Singha AS, Rana AK. A study on benzoylation and graft copolymerization of lignocellulosic fiber. *J Polym Environ.* 2012;20(2):361-371.
4. Person MD, Kash PW, Butler LJ. Nonadiabaticity and the competition between alpha and betabond fission upon  $[n,\pi^*(C=O)]$  excitation in acetyl- and bromoacetyl chloride. *Journal of Chemical Physics.* 1992;97(1):355-73.
5. Deshmukh S, Hess WP. Photodissociation of acetyl-chloride: Cl and CH<sub>3</sub> quantum yields and energydistributions. *Journal of Chemical Physics.* 1994;100(9):6429-33.
6. Shibata T, Suzuki T. Photofragment ion imaging with femtosecond laser pulses. *Chemical Physics Letters.* 1996;262(1-2):115-9.
7. Rowland B, Hess WP. UV photochemistry of thin film and matrix-isolated acetyl chloride by polarized FTIR. *Journal of Physical Chemistry.* 1997;101(43):8049-56.
8. Saha A, Kawade M, SenGupta S, Upadhyaya HP, Kumar A, Naik PD. Photodissociation dynamics of benzoyl chloride at 235 nm: Resonance-enhanced multiphoton ionization detection of Cl and HCl. *J Phys Chem.* 2014;118(7):1185-1195.
9. Tanaka N, Fujiwara H, Ogawa H, Nishikiori H. Matrix isolation studies of 185 nm light-induced cage reactions of o-chlorobenzaldehyde. *J Mol Struct.* 2012;1025:48-52.
10. Frisch MJ, Trucks GW, Schlegel HB, Scuseria GE, Robb MA, Cheeseman JR, Scalmani G, Barone V, Mennucci B, Petersson GA, Nakatsuji H, Caricato M, Li X, Hratchian HP, Izmaylov AF, Bloino J, Zheng G, Sonnenberg JL, Hada M, Ehara M, Toyota K, Fukuda R, Hasegawa J, Ishida M, Nakajima T, Honda Y, Kitao O, Nakai H, Vreven T, Montgomery Jr, J A, Peralta JE, Ogliaro F, Bearpark M, Heyd JJ, Brothers E, Kudin KN, Staroverov VN, Keith T, Kobayashi R, Normand J, Raghavachari K, Rendell A, Burant JC, Iyengar SS, Tomasi J, Cossi M, Rega N, Millam NJ, Klene M, Knox JE, Cross JB, Bakken V, Adamo C, Jaramillo J, Gomperts R, Stratmann RE, Yazyev O, Austin AJ, Cammi R, Pomelli C, Ochterski JW, Martin RL, Morokuma K, Zakrzewski VG, Voth GA, Salvador P, Dannenberg JJ, Dapprich S, Daniels AD, Farkas Ö, Foresman JB, Ortiz JV, Ciosowski JFox DJ. Gaussian 09, Revision D.01, Wallingford. Gaussian, Inc.; 2013.
11. Lee C, Yang W, Parr RG. Development of the colic-salvetti correlation-energy formula into a functional of the electron density. *Phys Rev B.* 1988;37(2):785-789.
12. Al-Jallo HN, Jalhood MG. Infrared spectra of aromatic acid halides. *Spectrochim Acta.* 1972;28:1655-1662.
13. Govindarajan M, Karabacak M, Udayakumar V, Periandy S. FT-IR, FT-raman and UV spectral investigation: Computed frequency estimation analysis and electronic structure calculations on chlorobenzene using HF and DFT. *Spectrochim Acta.* 2012;88:37-48.
14. Nagata M, Futami Y, Akai N, Kudoh S, Nakata M. Structure and infrared spectrum of 2-hydroxyphenyl radical. *Chem Phys Lett.* 2004;392(1-3):259-264.
15. Verma VN, Nair KPR, Srivastava MP. Ultraviolet absorption spectrum of benzoyl chloride in vapor phase. *Ind J Pure Appl Phys.* 1970;8(12):856-857.
16. Turro NJ, Ramamurthy V, Scaiano JC. *Modern molecular photochemistry of organic molecules.* Sausalito: University Science Books; 2010.

17. Xiao H, Maeda S, Morokuma K. CASPT2 study of photodissociation pathways of ketene. *J Phys Chem A*. 2013;117(32):7001-7008.

---

© 2014 Tanaka; This is an Open Access article distributed under the terms of the Creative Commons Attribution License (<http://creativecommons.org/licenses/by/3.0>), which permits unrestricted use, distribution, and reproduction in any medium, provided the original work is properly cited.

*Peer-review history:*

*The peer review history for this paper can be accessed here:  
<http://www.sciedomain.org/review-history.php?iid=536&id=7&aid=5312>*